International Journal of Thermofluids 22 (2024) 100605

Contents lists available at ScienceDirect

International Journal of Thermofluids

journal homepage: www.sciencedirect.com/journal/international-journal-of-thermofluids

A numerical study of multiphase flow boiling heat transfer of nanofluids in the horizontal metal foam tubes

Shahram Azizifar [a,*], Mengjie Song [b,c], Christopher Yu Hang Chao [d], Seyyed Hossein Hosseini [e], Libor Pekař [f,g]

[a] Faculty of Mechanical and Energy Engineering, Shahid Beheshti University, Tehran, Iran
[b] Department of Energy and Power Engineering, Beijing Institute of Technology, Beijing, China
[c] School of Mechanical Engineering, Hanyang University, 222 Wangsimni-Ro, SeongDong-Gu, Seoul, Korea
[d] Department of Building Environment and Energy Engineering and Department of Mechanical Engineering, the Hong Kong Polytechnic University, Hong Kong 999077, China
[e] Department of Chemical Engineering, Ilam University, 69315-516 Ilam, Iran
[f] Faculty of Applied Informatics, Tomas Bata University in Zlín, Nad Stráněmi 4511, 76005 Zlín, Czech Republic
[g] Department of Technical Studies, College of Polytechnics Jihlava, Tolstého 16, 58601 Jihlava, Czech Republic

A R T I C L E I N F O

Keywords:
Flow boiling
Copper metal foam
Mixture model
Nanofluid
Heat transfer
Pressure drop

A B S T R A C T

The study aims to numerically investigate the flow boiling of Al2O3/H2O and CuO/H2O nanofluids and water in pipes filled with copper metal foams. Four different values of porosity and three values of pore density have been used. To perform numerical simulation, the mixture model has been developed. For the first time, the effects of nanoparticle deposition on the wettability of heating surfaces were considered with the help of user-defined functions. Besides, the effect of metal foams with different porosities on the onset of nucleate boiling was evaluated. The thermal performance of metal foam pipes has been compared with each other by comparing the increase in heat transfer and pressure drop. As a result, by reducing the porosity from 0.95 to 0.80, the heat transfer coefficient was increased by 59 %, while the pressure drop increased by 28 %. Finally, by comparing the increase in heat transfer and pressure drop, results show that the metal foam pipe with 80 % porosity and 5 pores per inch has the best thermal performance. The results of this study are expected to be used for the optimization of advanced phase change cooling technologies.

1. Introduction

In some industrial systems, such as microchannels, geothermal reservoirs, and nuclear reactors, boiling processes and the mechanism of multiphase flows in porous media are observed. The significant increase in heat transfer coefficient during flow boiling compared to single-phase convection heat transfer makes the boiling process and multiphase heat transfer phenomenon particularly interesting for thermal researchers.

The use of nanofluids to improve the thermal conductivity of working fluids is an interesting research topic for passive heat transfer enhancement. [1,2]. Using nanofluids can both increase the flow boiling heat transfer coefficient [3,4] and weaken it [5,6]. Improving the thermophysical properties of nanofluids and surface wettability are the reasons for increasing heat transfer and changing the number of micro-cavities on the surface and wettability is the reason for the weakening of it. Other studies have found that nanofluids do not affect heat transfer [7,8].

The deposition of nanoparticles during the boiling process and their settling on the heated surface during boiling and bubble formation is one of the critical challenges of using nanofluids in boiling and multiphase heat transfer systems. This matter leads to an increase in the diameter of bubble departure, less interaction of bubbles with nanoparticles, reduction of nucleation sites, and ultimately improvement of wettability [9–11].

Broughton et al. [12] investigated water flow boiling in metal foam structures with steam paths experimentally and numerically. In their numerical modeling, a conjugate computational fluid dynamics and heat transfer (CFD-HT) model utilizing a three-dimensional volume of fluid (VOF) model with an accompanying evaporation/condensation model

Abbreviations: ppi, Pores per inch; htc, Heat transfer coefficient; onb, Onset of Nucleate Boiling; UDF, User Defined Function.

* Corresponding author.
E-mail address: s.azizifar1986@gmail.com (S. Azizifar).

https://doi.org/10.1016/j.ijft.2024.100605

Available online 13 February 2024

Nomenclature

C	Inertial coefficient
d	Diameter (m)
E	Energy (J)
F	Body force (N)
g	Gravity (m/s2)
H	Enthalpy (kJ/kg)
h	heat transfer coefficient (W/m2 K)
K	Permeability (A)
L	Latent heat (J/kg)
M	Molar mass (kg/mol)
P	Pressure (Pa)
q	Heat flux (kW/m2)
R	Gas constant
u	Velocity (m/s)

Greek symbols

α	Phase fraction
β	Accommodation coefficient
∇	Vector gradient operator
ε	Porosity
μ	Viscosity (kg/m s)
ρ	Density (kg/m3)
Φ	Volume fraction of phase

Superscripts

b	bubble
dr	Drift velocity
f	Fiber
po	Pore
k	Phase
l	Liquid
m	Mixture
s	Solid
sat	Saturated
in	Inner
w	Water

provided in-depth visualization of the boiling flow phenomena. The study shows that the thermohydraulic performance is better for the foam sample with dedicated vapor pathways than the uniform foam, across a range of heat fluxes, in terms of both pressure and heat transfer performance metrics.

Yeo and No [13] conducted a study on film boiling in chimney-structured porous media and heat pipes. They discovered that the density and pore size of the chimneys greatly affect the heat transfer performance in Corrosion Residual Unidentified Deposit (CRUD). The researchers also noted that there is an optimal number of chimneys required to achieve maximum performance.

The boiling process and multiphase heat transfer in porous media are mainly studied through experiments [14–21]. The flow boiling of nanofluids in a pipe filled with metal foam was investigated by Azizifar et al. [22]. It stated that metal foam enhances heat transfer by 3.5–5.8 times the plain pipe. However, nanofluids reduce the heat transfer coefficient (HTC) compared to water. They reported that the nanoparticles deposition on heated surfaces is responsible for the decrease in HTC of nanofluids.

In the numerical discussion, Li et al. [23] studied the transition behavior of fluid flow boiling in porous vertical channels. The minimum liquid saturated for the aiding flows occurs at the end of the heated section, while for the opposite flows, it is within the heated section and shifts upwards as the Peclet number decreases and the Rayleigh number increases. Samir and Hossein [24] investigated boiling natural convection of R-134a refrigerant in a porous vertical tube. In this study, they investigated flow behavior in transition and steady-state conditions. They stated that there is a minimum of liquid saturated at the end of the tube and that a dry-out point is always visible in the second half. In another numerical study, Sivasankaran and Mallawi [25] used a two-phase Eulerian model to investigate the flow boiling of CuO/H_2O inside a vertical metal foam tube. The foam was made of aluminum and had a porosity of 0.80 and a 10 PPI. They stated that in the single-phase flow, heat transfer coefficient (HTC) would double compared to a simple tube, although in two-phase flow, the HTC decreased and was about 25 % higher than a simple tube. In a sinusoidal metal foam channel, Nazari and Toghraie [26] studied CuO/H_2O heat transfer. The researchers stated that metal foam effectively increases the HTC. A numerical method was used by Lu et al. [27] to study the forced convection heat transfer in a metal foam heat exchanger. As concluded, the overall HTC is highly dependent on the porosity and pore density. Table 1 shows a summary of previous studies on flow boiling in metal foams.

Referring to the reported studies, it is clear that no research has been

Table 1
Studies have been conducted on flow boiling in metal foams.

Findings	Model	Geometry-Fluid	Researchers
25 % increase in flow boiling HTC compared to plain tube.	Eulerian-Eulerian	Vertical metal foam tube-CuO/H_2O	Sivasankaran and Mallawi [25]
Metal foam enhances HTC by 3.5–5.8 times the plain tube. Negative effect of nanofluids on heat transfer coefficient.	Experimental	Vertical metal foam tube-Water	Azizifar et.al. [22]
The overall HTC increases with porosity, pore density, mass flux and/or heat flux.	Eulerian-Eulerian	Horizontal metal foam tube- R134a	Lu and Zhao [28]
A metal foam tube with a moderate to low porosity with a high to moderate pore density is recommended.	Eulerian-Eulerian	Horizontal metal foam tube- R134a	Mohammad et al. [29]
The optimal filling ratio is 0.6, As the PPI and porosity increase, the HTC also increases.	Eulerian-Lagrangian	Filled foamed copper	
channel - Water	Shen [30]		
The liquid saturation will reach its minimum value at the exit, and the dry-out point will always be seen at the 2nd half of the tube length.	Multiphase Mixture model	Vertical metal foam tube-R134a	Samir and Hussain [24]
The results show that HTC has almost doubled by reducing the cell size from 20 ppi to 40 ppi for a given porosity.	Experimental	Horizontal metal foam tube- R134a	Zhao et al. [17]

done on flow boiling of Al_2O_3/H_2O and CuO/H_2O nanofluids in pipes filled with copper that consider the effects of different porosities and pore densities on heat transfer coefficient and pressure drop. Also, as far as the authors know, the effect of metal foam on the onset of nucleate boiling (ONB), which has been shown experimentally in previous works [20–22], has not been studied in numerical simulations. In addition, through user-defined functions (UDF) codes, the effect of nanoparticle deposition, is studied in metal foam pipes for the first time. To demonstrate the impact of the new model used in this study, which accounts for the deposition of nanoparticles on the heated surface and the improvement of wettability, a comparison was made between the heat transfer coefficient of this model and the modeling results of [29]. This comparison was made considering the experimental results of [22]. Besides, the thermal performance of different metal foams has been evaluated.

2. Methodology

2.1. Assumptions

The tubes filled with copper metal foam placed horizontally 1000 mm long and 10 mm in diameter are considered the geometry under consideration. Metal foam improves heat transfer by increasing the contact surface, and the effective thermal conductivity [26]. As the nanofluids pass through the tube, they absorb the heat caused by applying a heat flux on the tube surface, and the boiling process occurs. Viscosity and inertia losses due to metal foam cause a pressure loss. In this study, the following assumptions are used to perform the numerical procedure [29].

i. The density changes are calculated based on the Boussinesq approximation,
ii. Metal foam is considered a homogeneous and isotropic material,
iii. It is assumed that the fluids phases and metal foam have a thermal equilibrium condition,
iv. Nanofluids are assumed to be stable in the analysis.

2.2. Nnaofluids: Thermophysical properties

The following relationships are used for density and specific heat [31].

$$\rho_{nf} = \lambda\rho_{np} + (1-\lambda)\rho_{bf} \tag{1}$$

$$C_{p,nf} = \frac{\phi\rho_{np}C_{p,np} + (1-\phi)\rho_{bf}C_{p,bf}}{\rho_{nf}} \tag{2}$$

In the above relationships, ρ_{np} is the nanoparticles density, ρ_{bf} is the base fluid density, λ is nanoparticles volume fraction, and the $C_{p,np}$, $C_{p,bf}$ are specific heats of nanoparticles and base fluid, respectively. According to [32], the thermal conductivity and viscosity of Al_2O_3/H_2O nanofluid can be determined using the following relationships.

$$\frac{k_{nf}}{k_{bf}} = 4.97\lambda^2 + 2.72\lambda + 1 \tag{3}$$

$$\frac{\mu_{nf}}{\mu_{bf}} = 123\lambda^2 + 7.3\lambda + 1 \tag{4}$$

The following relationships are used for CuO/H_2O nanofluid [32].

$$\frac{k_{nf}}{k_{bf}} = 28.905\lambda^2 + 2.827\lambda + 1 \tag{5}$$

$$\frac{\mu_{nf}}{\mu_{bf}} = 0.009\lambda^3 + 0.051\lambda^2 - 0.319\lambda + 1.475 \tag{6}$$

Table 2 shows the thermophysical properties of nanoparticles.

2.3. Mixture model

The two-phase mixture model is a simple and functional model . This model is widely used to simulate liquid-gas and liquid-solid flows. The governing with a steady-state flow condition are as follows [33]:

Continuity:

$$\nabla.\rho_m \vec{u}_m = 0 \tag{1a}$$

$$\vec{u}_m = \frac{\sum_{k=1}^{2}\alpha_k\rho_k\vec{u}_k}{\rho_k} \tag{2a}$$

$$\rho_m = \sum_{k=1}^{2}\alpha_k\rho_k \tag{3a}$$

Momentum:

$$\frac{1}{\varepsilon}\nabla.\left(\rho_m\vec{u}_m\vec{u}_m\right) = -\nabla P + \frac{1}{\varepsilon}\nabla.\left[\mu_m\left(\nabla\vec{u}_m + \nabla\vec{u}_m^{T}\right)\right] + \varepsilon\rho_m g + \varepsilon\nabla.\left(\sum_{k=1}^{2}\alpha_k\rho_k\vec{u}_{dr,k}\vec{u}_{dr,k}\right) + \vec{F} \tag{4a}$$

In Eq. (4), term $\vec{F}$ is due to the presence of metal foam in the pipe [34]:

$$\vec{F} = \left(\frac{\mu_f}{K} + \frac{\rho_f C|u|}{\sqrt{K}}\right)\vec{u} \tag{5a}$$

$$C = 0.00212(1-\varepsilon)^{-0.132}\left(\frac{d_f}{d_{po}}\right)^{-1.63} \tag{6a}$$

$$\frac{K}{d_{po}^2} = 0.00073(1-\varepsilon)^{-0.224}\left(\frac{d_f}{d_{po}}\right)^{-1.11} \tag{7}$$

$$d_{po} = \frac{0.0254}{PPI} \tag{8}$$

$$\frac{d_f}{d_{po}} = 1.18\sqrt{\frac{(1-\varepsilon)}{3\pi}}\left(\frac{1}{1-\exp(-(1-\varepsilon)/0.04)}\right) \tag{9}$$

Energy:

$$\nabla.\sum_{k=1}^{2}\left(\alpha_k\vec{u}_k(\rho_k E_k + p)\right) = \nabla.\left(k_{eff}\nabla T\right) + S_E \tag{10}$$

$$E_k = H_k - \frac{P}{\rho_k} + \frac{u_k^2}{2} \tag{11}$$

In Eq. (10), the term S_E represents an energy source. Also, k_{eff} is considered as the effective thermal conductivity of metal foam and fluid, which is calculated by Eq. (12).

$$k_{eff} = (1-\varepsilon)k_s + \varepsilon k_w \tag{12}$$

The equation for the vapor phase, which is considered the second phase and is used to calculate the volume of the phrase, is as follows:

$$\nabla.\left(\alpha_v\rho_v\vec{u}_m\right) = -\nabla.\left(\alpha_v\rho_v\vec{v}_{dr,v}\right) + S_M \tag{13}$$

In Eq. (13), the term S_M indicates a source of mass. The source terms of S_M and S_E are based on the equations defined by Lee et al. [35], which have been validated in many references, including [36–38], in this paper applied as UDFs in ANSYS-Fluent software.

$$S_M = \begin{cases} 0 & T_l < T_{sat} \\ \in\phi_l\rho_l\dfrac{T_l - T_{sat}}{T_{sat}} & T_l \geq T_{sat} \end{cases} \tag{14}$$

$$S_E = -\in\phi_l\rho_l\left|\frac{T_l - T_{sat}}{T_{sat}}\right|\Delta h_{fg} \tag{15}$$

Table 2
Thermophysical properties of Al_2O_3 and CuO nanoparticles.

Nanoparticle	ρ (kg/m³)	c_p (J/kg K)	k (W/m K)
Al_2O_3	3890	525	17.65
CuO	6400	540	32.9

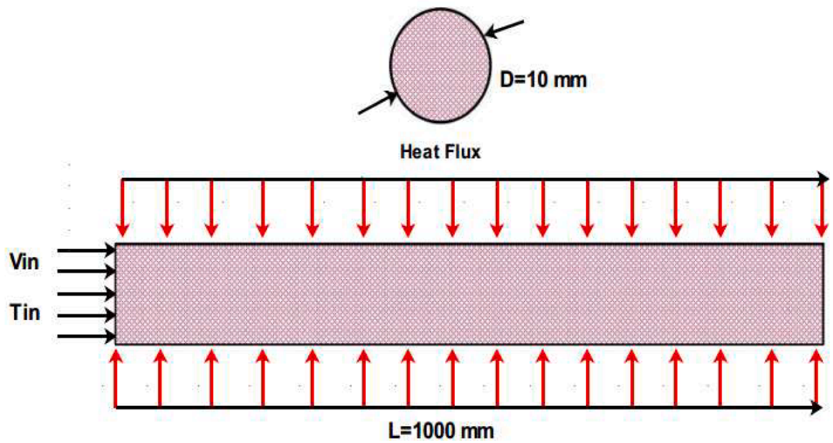

Fig. 1. The schematic diagram of the metal foam tube.

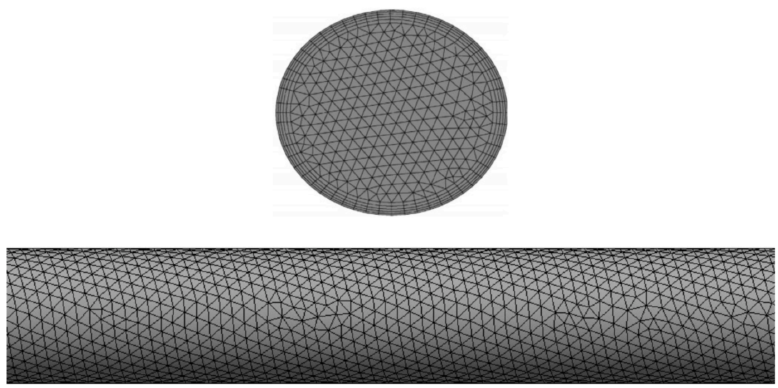

Fig. 2. Generated mesh to solve equations in the metal foam pipe.

In Eqs. (14) and (15) $\in$ is a time relaxation factor considered in the form of Eq. (16).

$$\in = \frac{6}{d_b}\beta\sqrt{\frac{M}{2\pi RT_{sat}}}L\left(\frac{\phi_v\rho_v}{\rho_l-\rho_v}\right) \tag{16}$$

Since the correlations for calculating bubble diameter are based on water, their application to simulating the boiling of nanofluids is open to question. Li et al. [39] current correlation is used to calculate bubble diameter. Li et al. [39] proposed the following equation taking into account the deposition of nanoparticles during boiling.

$$d_{bd} = 0.626977\frac{2+3\cos\theta-\cos^3\theta}{4}\left[\frac{\sigma}{g(\rho_l-\rho_g)}\right]^{0.5} \tag{17}$$

where θ is the liquid contact angle with the heated surface. The effects of the dispersed gas bubbles on the turbulence in the continuous liquid phase are modelled by introducing appropriate source terms in the k-ε equation. The standard k-ε, turbulence model is used for modelling the boiling fluid considering turbulence kinetic energy (k) and dissipation rate (ε). This model, is suitable for simulating fully turbulent flows. Also, the model should have acceptable accuracy near walls. For this purpose, the standard wall function has been used. The overall HTC in the boiling process is considered as follows:

Table 3
The study of the generated mesh.

Element No.	391,741	672,184	895,432	1,629,408	3,443,721
h (W/m^{2}K)	19,427	20,895	22,011	30,625	30,590
ΔP(Pa)	32,921	33,431	35,943	49,500	49,112

$$h = \frac{q}{T_{s,in} - T_{b,nf}} \tag{18}$$

2.4. Geometry, boundary conditions, and fluid's thermal properties

As said above, the considered geometry is a horizontal tube with a length of 1000 mm, and an inner diameter of 10 mm.

The boundary conditions in this study are as follows:

At the inlet of the pipe, the condition of inlet velocity and temperature is applied; at the outlet of the pipe, the condition of relative pressure is zero. Different values of applied heat flux were examined in the pipe wall. (Fig. 1).

2.5. Meshing and numerical approach

The desired geometry is considered horizontally. Near the inner wall of the pipe, as well as at the inlet and outlet of the pipe, where the gradients of velocities and temperature are intense, the mesh is more delicate than elsewhere. An unstructured mesh is used to discretize computational geometry. Fig. 2 shows the mesh used in this paper. The equations are discretized using the control volume and double-precision method in ANSYS-Fluent software, and to solve the coupled velocity-pressure equations, the SIMPLE method is used. Also, to correct the momentum equation, the Presto scheme, and the energy equation, the QUICK scheme is used. The convergence criteria for the continuity, momentum, and energy equations are 10^{-4}, 10^{-6}, and 10^{-6}, respectively. To ensure the independence of the mesh, several different meshes have been used, which in Table 2 can be seen as the effect of different meshes on the HTC and pressure drop.

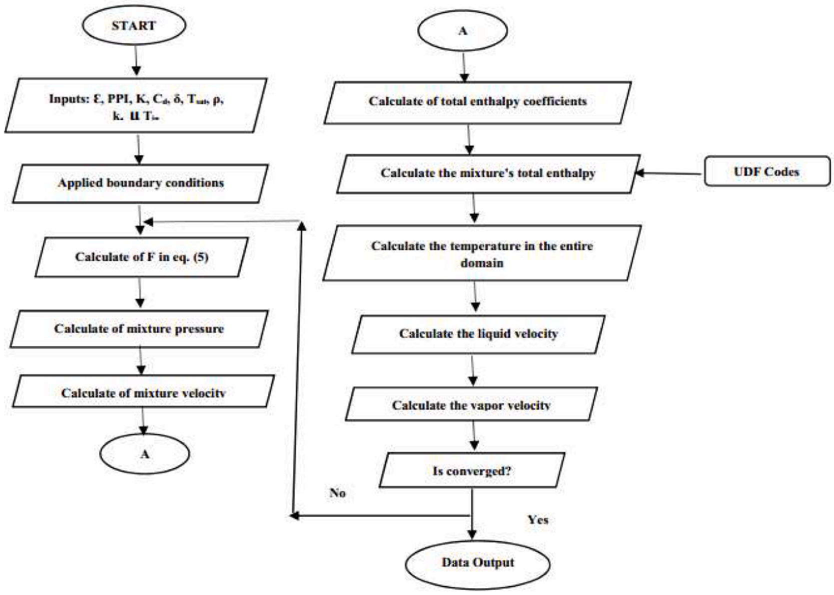

Fig. 3. Flowchart of solution procedure.

Table 4
The parameters used in the simulation results and the values for [22].

	ε	PPI	k_f (W/m K)	μ (Pa s)	Permeability	d_f (mm)	d_{po} (mm)
Exp [22]	0.80	10	–	–	1.89×10^{-8}	0.80	2.60
Simulation	0.80	10	0.653	0.0003779	1.89×10^{-8}	0.80	2.60

By referring to Table 3, with the increase in the number of elements from 1629408 to 3443721, the changes in HTC and pressure drop are minimal (less than 1 %), therefore, the number of 1629408 cells is selected.

Fig 3 illustrates the flowchart used to solve the problem in this study.

3. Results and discussions

In this section, the results of numerical simulation of flow boiling of Al_2O_3/H_2O, CuO/H_2O nanofluids, and water are discussed. For this purpose, first, the numerical simulation results performed in ANSYS-Fluent are validated by comparing with experimental results of [20] both in terms of the HTC and pressure drop. Then, the effects of different porosities ($\varepsilon = 0.8, 0.85, 0.9, 0.95$) and pore densities (5, 10, 20 PPI) on HTC and pressure drop, are discussed.

3.1. Validation

The study of [22] is an experimental investigation of HTC and pressure drop of water and Al_2O_3/H_2O, CuO/H_2O nanofluids flow boiling in a horizontal metal foam tube. The test section was a circular tube made of stainless steel 304. It had an inner diameter of 10 mm, a wall thickness of 1.0 mm, and an effective length of 1000 mm. The tubes were filled with open-cell metal foam made of copper, which had a porosity of 0.80 and a pore density of 10-PPI. (Table 4).

Tables (5), and (6) compare numerical results and experimental results of [22] for Al_2O_3/H_2O, and CuO/H_2O nanofluids related to HTC, respectively.

As can be seen in Tables 5 and 6, the numerical model can predict the HTC of Al_2O_3/H_2O and CuO/H_2O nanofluids with acceptable accuracy. Figs. 4 and 5 display the results of pressure drop for Al_2O_3/H_2O and CuO/H_2O nanofluids, respectively. As can be seen, numerical modeling can predict pressure drop with reasonable accuracy. With the increase in mass flux, the pressure drop increases. The numerical model can predict the pressure drop with reasonable accuracy. The maximum error of the numerical simulation is about 16 %, which is obtained at a mass flux of 290 kg/m^2s.

3.2. Temperature and pressure distribution

To understand the effect of metal foam on HTC and pressure drop, first, the temperature and pressure distribution throughout different contours are displayed. Fig. 6 indicates the temperature distribution along the pipe with a porosity of 0.90, 5 PPI, T_{in}=58 °C, $G = 210$ kg/m^2s, and $q = 66$ kW/m^2 for Al_2O_3/H_2O nanofluid.

By referring to Fig. 6, at the inlet of the pipe, a single-phase fluid flow is established. As the nanofluid flows along the tube, more heat has transferred to it through the wall of the tube and the metal foam, and

Table 5
The HTC comparison of simulation results and experimental of [22] for Al_2O3/H_2O.

T_{in} (°C)	q (kW/m^2)	G (kg/m^2s)	h_{exp} (kW/m^2 K) [22]	h_{sim} (kW/m^2 K)	Err (%)
45	80	145	10.80	11.87	9
50	80	210	11.05	12.41	11
50	80	145	7.20	7.93	9
50	150	240	16.08	17.86	10

Table 6
The HTC comparison of simulation results and experimental of [22] for CuO/H_2O.

T_{in} (°C)	q (kW/m^2)	G (kg/m^2s)	hexp (kW/m^2 K) [22]	h_{sim} (kW/m^2 K)	Err (%)
45	80	145	11.40	12.39	8
50	80	210	12.60	14.02	10
50	80	145	7.12	7.92	10
50	150	240	17.20	18.90	9

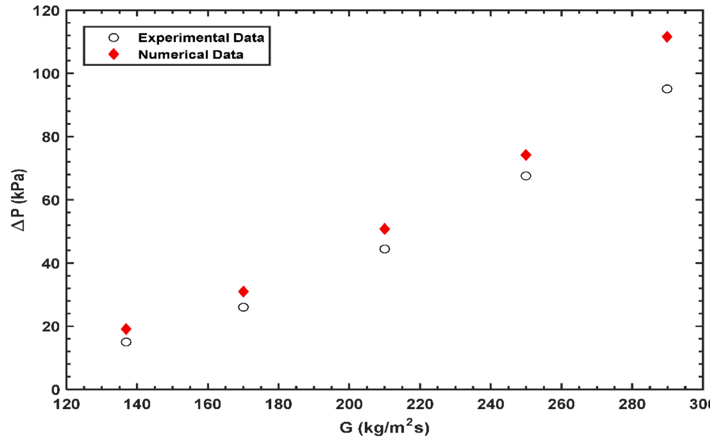

Fig. 4. Comparison of simulation and experimental results [22] related to pressure drop for Al_2O_3/H_2O.

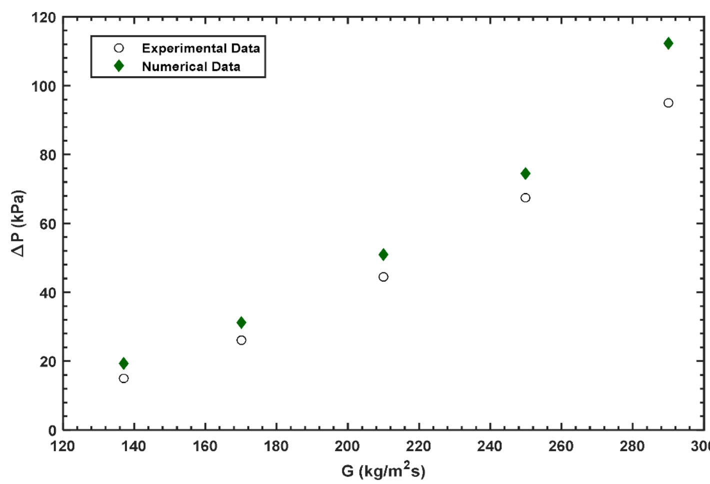

Fig. 5. Comparison of simulation and experimental results [22] related to pressure drop for CuO/H_2O.

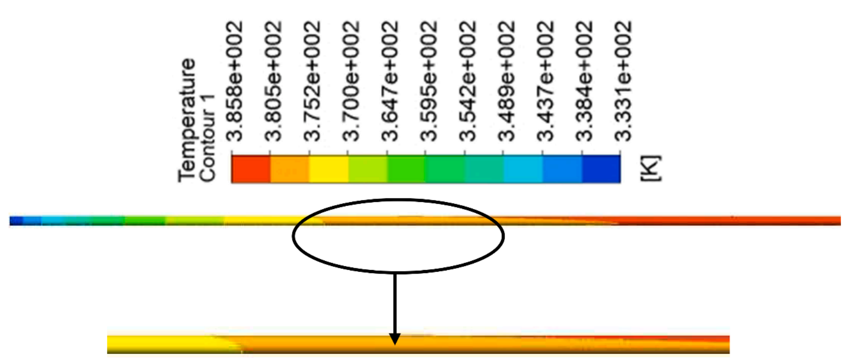

Fig. 6. Temperature distribution contour of Al_2O_3/H_2O nanofluid for ε= 0.90, 5 PPI, T_{in} = 58 °C, G = 210 kg /m^{2}s, q = 66 kW/m^2.

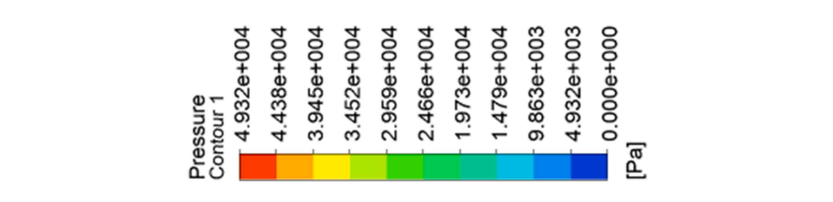

Fig. 7. Pressure distribution contour of Al_2O_3/H_2O nanofluid for ε= 0.80, 5 PPI, T_{in} = 50 °C, G = 210 kg /m^{2}s, q = 80 kW/m^2.

gradually, as the nanofluid temperature near the wall goes excess the saturation temperature, 100 °C, the boiling process begins, and bubbles begin to form.

Fig. 7 demonstrates the pressure distribution contour of Al_2O_3/H_2O nanofluid along the metal foam tube (ε = 0.80, 5 PPI) for boundary conditions of T_{in}=50 °C, G = 210 kg/m^{2}s, and q = 80 kW/m^2. At the beginning of the pipe (left side), where the single-phase flow is dominant, the pressure drop is significant. As the nanofluid advances along the tube and absorbs the heat, the boiling process begins, and bubbles begin to form; the pressure drop at the end of the tube is less.

3.3. The effect of metal foam's porosity on the ONB

Fig. 8 the vapor volume fraction for two different porosity of 0.85 and 0.95 with 5 PPI for T_{in} = 58 °C, G = 210 kg /m^{2}s, q = 66 kW/m^2 for Al_2O_3/H_2O. Considering the contours shown in Fig. 8 for both porosities, it is determined that in a metal foam pipe withε = 0.85, the ONB occurs at a distance of z = 33.50 cm from the tube's inlet. While withε = 0.95, boiling occurs from a distance of z = 31.56 cm.

Fig. 8 indicates that higher porosity results in boiling starting closer to the pipe inlet. In other words, the higher the porosity, the closer the metal foam pipe is to a simple pipe. Experimental results [20,21] reveal that boiling begins earlier in a simple tube than in a metal foam tube. Similarly, in a metal foam tube with higher porosity, boiling begins earlier.

3.4. Effect of different porosities

Fig. 9 illustrates the changes in HTC for three different heat fluxes and T_{in} = 58 °C, G = 210 kg /m^{2}s, and 5 PPI for Al_2O_3/H_2O nanofluid. According to Fig. 9, as the porosity increases, the HTC decreases. In other words, with increasing porosity, the contact surface decreases (the specific surface area of metal foam decreases and consequently thermal conductivity decreases), thus the HTC also decreases. This behavior of HTC in terms of porosity is in good agreement with the results of Zhang et al. [40] and Qu et al. [41].

Fig. 10 reveals the results related to pressure drop in terms of porosity for T_{in}=58 °C, G = 210 kg/m^{2}s, q = 66 kW/m^{2}K, and 5 PPI for all working fluids. As expected, with increasing the porosity, the pressure drop decreases, which is due to the reduction of the solid structure of the metal foam and thus reduces the resistance in the fluid flow path. Also, although there is a slight difference between pressure drop of water and nanofluids, due to the higher thermophysical properties, such as the viscosity, and density of nanofluids compared to water. Table 7 shows the changes in the HTC and pressure drop for T_{in} = 58 °C, G = 210 kg /m^{2}s, q = 66 kW/m^2, and pore density 5 PPI.

By referring to Table 7, it can be found that with decreasing porosity, HTC and also pressure drop increase. However, the increase in HTC is more significant than the increase in pressure drop. For example, by reducing the porosity from 0.95 to 0.80, for Al_2O_3/H_2O, the HTC increases by approximately 59 %, while the pressure drop increases by 28 %. Therefore, a metal foam with a porosity of 0.80 has a better thermal performance than others. Also, the HTC of nanofluids is slightly higher than water, for example; for CuO/H_2O nanofluids it is about 5 % higher than water in the best case.

3.5. Effect of different pore densities (PPIs)

In Fig. 11, changes in HTC of Al_2O_3/H_2O in terms of porosity for three different values of pore density (PPIs) for T_{in} = 58 °C, G = 210 kg/m^{2}s, q = 51 kW/m^2 is displayed.

As the pore density increases (average pore diameter decreases), the HTC increases, which can be due to the increase in the specific contact surface and, consequently, the increase in the effective thermal conductivity. For example, for a porosity of 0.80, by increasing the pore density from 5 PPI to 20 PPI, the HTC increases by 4.7 %. Buonomo et al. [42], in a numerical study, showed that increasing the pore density has a negligible effect on the HTC. Also, Arbak et al. [43], in an experimental

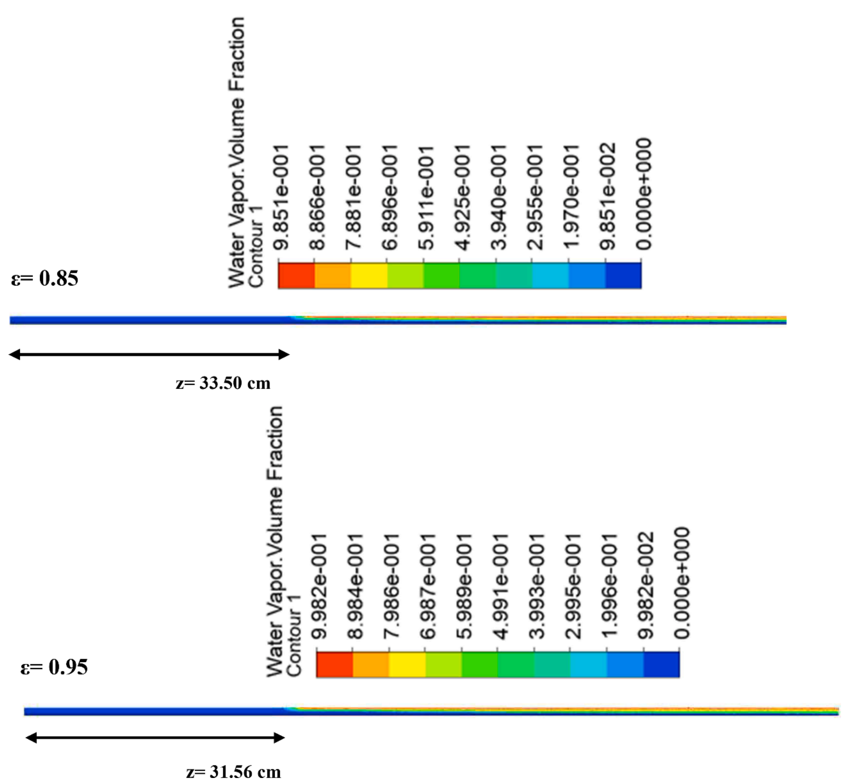

Fig. 8. Vapor volume fraction contours for 5 PPI, T_{in} = 58 °C, G = 210 kg/m^{2}s, q = 66 kW/m^2.

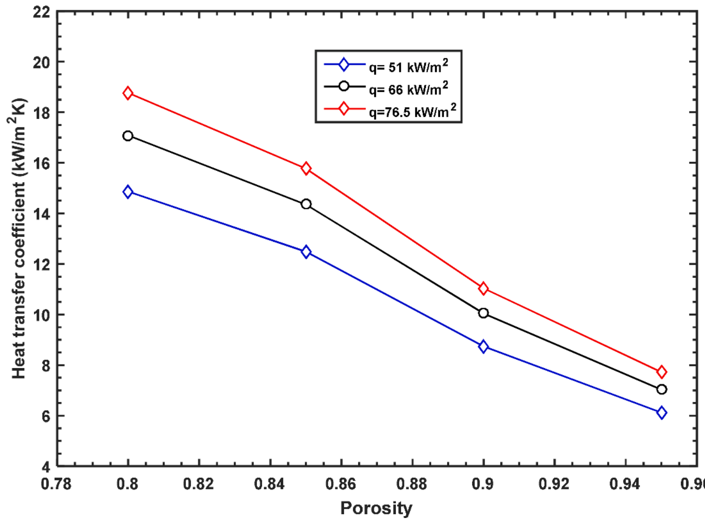

Fig. 9. Changes in the HTC according to porosity and 5 PPI for Al_2O_3/H_2O nanofluid.

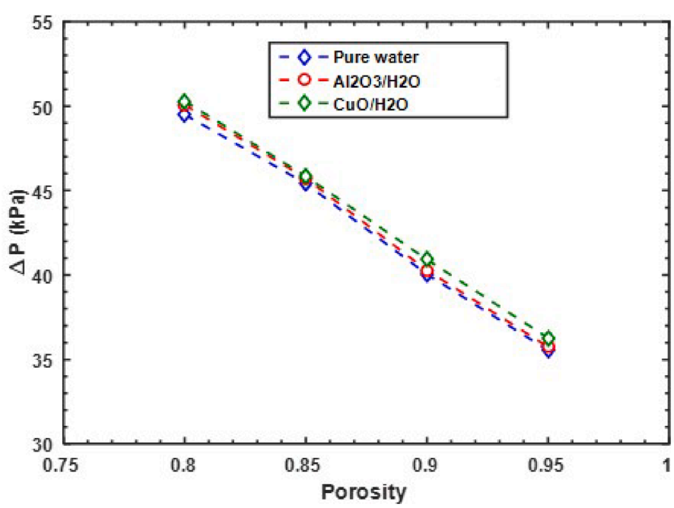

Fig. 10. Variation of the pressure drop as a function of porosities for 5 PPI.

Table 7
The effect of different porosity on HTC and pressure drop.

	CuO/H_2O		Al_2O_3/H_2O		H_2O	
ΔP (kPa)	h(kW/ m^2K)	ΔP (kPa)	h(kW/ m^2K)	ΔP (kPa)	h(kW/ m^2K)	Porosity
50.94	17.74	50.80	17.08	49.50	16.70	0.80
45.85	14.90	45.72	14.35	45.42	14.03	0.85
40.92	10.43	40.28	10.04	40.04	9.82	0.90
36.28	7.30	35.75	7.03	35.55	6.90	0.95

study, stated that metal foam with 10 PPI has a better HTC than 20 PPI. The pressure drop changes in terms of porosity for different values of pore densities are displayed in Fig. 12.

By increasing the pore density from 5 PPI to 20 PPI, the pressure drop significantly increases from 50.80 kPa to 267.11 kPa, because the number of ligaments and metal foam constraints in the fluid flow path increases too, and, consequently, the pressure drop increases. Table 8 reveals the changes in HTC and pressure drop for different values of pore density for $T_{in} = 58$ °C, $G = 210$ kg/m^{2}s, $q = 66$ kW/m^2 and porosity of 0.80. According to Table 8, for Al_2O_3/H_2O nanofluid, with increasing pore density (decreasing average pore diameter), the HTC and the pressure drop increase, although the rate of increase of HTC compared to the pressure drop is negligible. As the pore density increases from 5 PPI to 20 PPI, the HTC increases by approximately 4.7 %, while the pressure drop increases by 435 %. Therefore, a metal foam with 5 PPI is preferable to others.

3.6. Evaluation of the new simulation method used in this study

This study considers the deposition of nanoparticles on a heated surface to improve its wettability, which is a novel aspect. One of the challenges in using nanofluids in boiling (both pool boiling and flow boiling) is the deposition of nanoparticles on heated surfaces. Table 8 displays the results related to predicting the heat transfer coefficient based on simulation results [29] and the new method used in this article based on experimental results [22] for Al_2O_3/H_2O.

By referring to Table 9, it can be seen that the use of simulation in this article improves the prediction of the heat transfer coefficient by 6 to 7 percent compared to the used method [29].

4. Conclusion

The numerical simulation flow boiling of Al_2O_3/H_2O, CuO/H_2O nanofluids, and water in horizontal pipes filled with copper metal foam is investigated. Using the mixture model and user-defined functions in ANSYS-Fluent software, a simulation is performed. Besides, considering the nanoparticles deposition, the bubbles' diameter in the nanofluids' boiling has been calculated based on the Lee et al. [35] correlation and using user-defined functions. After verifying the numerical results, the effect of different porosity, as well as different pore densities on HTC and pressure drop, were investigated. In the numerical study, metal foam pipes with porosities of (ε = 0.80,0.85,0.90,0.95), and pore density of 5, 10, and 20 pores per inch were investigated. The following are the results of the numerical simulation.

1) Numerical simulation results showed that using metal foam with higher porosity leads to the onset of nucleate boiling and the formation of bubbles at a location closer to the inlet of the pipe.
2) At lower porosities, both heat transfer coefficient and pressure drop increase. For example, by reducing the porosity from 0.95 to 0.80, the heat transfer coefficient increased by 59 %, while the pressure drop increased by 28 %. Therefore, using metal foam with a porosity of 0.80 has a better thermal performance.

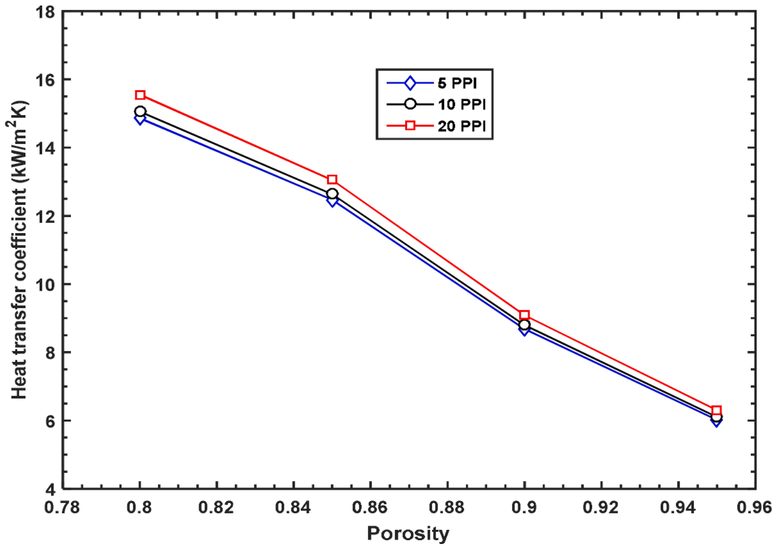

Fig. 11. Changes in HTC of Al_2O_3/H_2O in terms of porosity for different values of pore density.

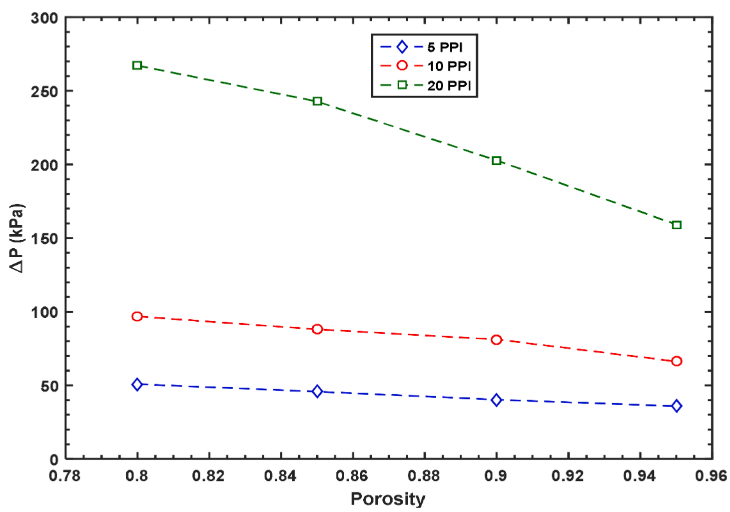

Fig. 12. Changes in pressure drop of Al_2O_3/H_2O in terms of porosity for different values of pore density.

Table 8
The effect of different pore densities on HTC and pressure drop (porosity of 0.80).

	CuO/H_2O		Al_2O_3/H_2O		H_2O	
ΔP (kPa)	h(kW/ m^2K)	ΔP (kPa)	h(kW/ m^2K)	ΔP (kPa)	h(kW/ m^2K)	PPI
50.94	17.74	50.80	17.08	49.50	16.70	5
96.96	17.98	96.76	17.30	96.20	16.92	10
270.04	18.57	267.11	17.89	265.59	17.48	20

3) As the pore density increases (decreasing average pore diameter), the heat transfer coefficient and the pressure drop increase. However, the increase in heat transfer coefficient is insignificant compared to the pressure drop.
4) A comparison of the results related to heat transfer coefficient and pressure drop of different porosities (ε = 0.80,0.85,0.90,0.95) and pore density of 5, 10, and 20 showed that metal foam with porosity of 0.80 and 5 pores per inch has better thermal performance.

Table 9
Comparison of simulation results used in this study with simulation results [29] for Al_2O_3/H_2O.

Current study	Sim [29]	Exp [22]		Boundary Condition	
Error (%)	h (kW/ m^2K)	Error (%)	h (kW/ m^2K)	h (kW/ m^2K)	
9	11,870	16	12,855	10,800	T_{in}= 45 (°C), q = 80 kW/m^2, G = 145 kg/m^2s
11	12,410	17	13,318	11,050	T_{in}= 50 (°C), q = 80 kW/m^2, G = 210 kg/m^2s
10	17,860	16	19,142	16,080	T_{in}= 50 (°C), q = 150 kW/m^2, G = 240 kg/m^2s

5) The simulation method used in this paper improves the prediction of the heat transfer coefficient by 6 to 7 percent compared to previous studies.

According to the simulation model in this article, the following suggestions for further work can be made:

- Numerical simulation of flow boiling of nanofluids in metal foams, assuming nonequilibrium thermal conditions between foam and fluid phases.
- Comparing the results of using dimple tubes and metal foam tubes to simulate the flow boiling of nanofluids.

CRediT authorship contribution statement

Shahram Azizifar: Writing – review & editing, Writing – original draft, Software, Formal analysis. **Mengjie Song:** Writing – review & editing, Software. **Christopher Yu Hang Chao:** Formal analysis, Data curation. **Seyyed Hossein Hosseini:** Software, Investigation, Data curation. **Libor Pekař:** Writing – review & editing, Formal analysis.

Declaration of competing interest

The authors declare that they have no known competing financial interests or personal relationships that could have appeared to influence the work reported in this paper.

Data availability

No data was used for the research described in the article.

Acknowledgments

The authors would like to acknowledge the Department of Physics, Collage of Education, University of Garmian, Kurdistan, Iraq for their support and contribution to this study. This research was funded by the National Natural Science Foundation of China (Grant No. 52076013), the Beijing Municipal Science & Technology Commission (Grant No. 3212024), the China-South Korea Youth Scientists Exchange Program in 2023 supported by the Ministry of Science and Technology of China and Ministry of Science and ICT of the Republic of Korea, and the National Research Foundation of Korea in 2023.

References

[1] Lin, Li-Wen, Corporate social and environmental disclosure in emerging securities markets, NCJ Int.' L. Com. Reg.. 35 (2009): 1.
[2] N. Dukhan, Forced convection of nanofluids in metal foam: an essential review, Int. J. Therm. Sci. 187 (2023) 108156.
[3] M.S. Kamel, F. Lezsovits, Enhancement of pool boiling heat transfer performance using dilute cerium oxide/water nanofluid: an experimental investigation, Int. Commun. Heat and Mass Transf. 114 (2020) 104587.
[4] P. Ashutosh, S.K. Ghosh, Surface qualitative analysis and ANN modelling for pool boiling heat transfer using Al2O3-water based nanofluids, Colloids Surf. A: Physicochem. Eng. Aspects 610 (2021) 125926.
[5] S.J. Kim, Pool Boiling Heat Transfer Characteristics of Nanofluids, Massachusetts Institute of Technology, Cambridge, MA, 2007. PhD thesis.
[6] Y. Wang, et al., A mechanism of heat transfer enhancement or deterioration of nanofluid flow boiling heat transfer, Int. J. Heat Mass Transf. 158 (2020) 119985.
[7] S.J. Kim, T. McKrell, J. Buongiorno, L.W. Hu, Subcooled flow boiling heat transfer of dilute alumina, zinc oxide, and diamond nanofluids at atmospheric pressure, Nucl. Eng. Des. 240 (2010) 1186–1194.
[8] P. Vassallo, R. Kumar, S. D'Amico, Pool boiling heat transfer experiments in silica-water nano-fluids, Int. J. Heat Mass Transf. 47 (2004) 407–411.
[9] D. Wen, Y. Ding, Experimental investigation into the pool boiling heat transfer of aqueous based γ-alumina nanofluids, J. Nanoparticle Res. 7 (2005) 265–274.
[10] J. Barber, D. Brutin, L. Tadrist, A review on boiling heat transfer enhancement with nanofluids, Nanoscale Res. Lett. 6 (2011) 1–16.
[11] S. Vafaei, T. Borca-Tasciuc, Role of nanoparticles on nanofluid boiling phenomenon: nanoparticle deposition, Chem. Eng. Res. Des. 92 (2014) 842–856.
[12] Justin Broughton, Emanuel Torres, Akshith Narayanan, Y.K. Joshi, Experimental and numerical investigation of flow boiling in additive manufactured foam structures with vapor pathways, ASME J. Heat Mass Transf. 146 (2024) 2.
[13] D.Y. Yeo, H.C. No, Modeling film boiling within chimney-structured porous media and heat pipes, Int. J. Heat Mass Transf. 124 (2018) 576–585.
[14] W.H. Hsieh, J.Y. Wu, W.H. Shih, W.C. Chiu, Experimental investigation of heat transfer characteristics of aluminum-foam heat sinks, Int. J. Heat Mass Transf. 47 (2004) 5149–5157.
[15] N.K. Choon, A. Chakraborty, S.M. Aye, W. Xiaolin, New pool boiling data for water with copper-foam metal at sub-atmospheric pressures: experiments and correlation, Appl. Therm. Eng. 26 (2006) 1286–1290.
[16] M.J. Song, Z.Y. Jiang, J. Shen, C.B. Dang, Y.Y. Jiang, Mathematical modeling investigation on flow boiling and high efficiency heat dissipation of two rectangular radial microchannel heat exchangers, Int. J. Heat Mass Transf. 190 (2022) 122736.
[17] C.Y. Zhao, W. Lu, S.A. Tassou, Flow boiling heat transfer in horizontal metal-foam tubes, J. Heat Transf. 131 (2009) 121002–1210010.
[18] A.A. Sertkaya, K. Altınısık, K. Dincer, Experimental investigation of thermal performance of aluminum finned heat exchangers and open-cell aluminum foam heat exchangers, Exp. Therm. Fluid Sci. 36 (2012) 86–92.
[19] R. Irwansyah, N. Putra, Pool boiling of nanofluids in vertical porous media, Appl. Mech. Mater. 388 (2013) 18–22.
[20] S. Azizifar, M. Ameri, I. Behroyan, An experimental study of subcooled flow boiling of water in the horizontal and vertical direction of a metal-foam tube, Therm. Sci. Eng. Prog. (2020) 100748.
[21] S. Azizifar, M. Ameri, I. Behroyan, Subcooled flow boiling of water in a metal-foam tube: an experimental study, Int. Commun. Heat Mass Transf. 118 (2020) 104897.
[22] S. Azizifar, M. Ameri, I. Behroyan, Experimental investigation of the subcooled flow boiling heat transfer of water and nanofluids in a horizontal metal foam tube, Heat Mass Transf. 57 (2021) 1499–1511.
[23] H.Y. Li, K.C. Leong, L.W. Jin, J.C. Chai, Transient behavior of fluid flow and heat transfer with phase change in vertical porous channels, Int. J. Heat Mass Transf. 53 (2010) 5209–5222.
[24] Ali Samir, I.Y. Hussain, Simulation of natural convection boiling heat transfer for refrigerant R-134a flow in a metal foam filled vertical tube, Case, Stud. Therm. Eng. 13 (2019) 100390.
[25] S. Sivasankaran, Fouad OM Mallawi, Numerical study on convective flow boiling of nanoliquid inside a pipe filling with aluminum metal foam by two-phase model, Case, Stud. Therm. Eng. 26 (2021) 101095.
[26] S. Nazari, D. Toghraie, Numerical simulation of heat transfer and fluid flow of Water-CuO Nanofluid in a sinusoidal channel with a porous medium, Phys. E: Low-Dimens. Syst. Nanostruct. 87 (2017) 134–140.
[27] W. Lu, C.Y. Zhao, S.A. Tassou, Thermal analysis on metal-foam filled heat exchangers. Part I: metal-foam filled pipes, Int. J. Heat Mass Transf. 49 (2006) 2751–2761.
[28] Wei Lu, Chang-Ying Zhao, Numerical modelling of flow boiling heat transfer in horizontal metal-foam tubes, Adv. Eng. Mater. 11 (10) (2009) 832–836.
[29] H.I. Mohammed, P.T. Sardari, D. Giddings, Multiphase flow and boiling heat transfer modelling of nanofluids in horizontal tubes embedded in a metal foam, Int. J. Therm. Sci. 146 (2009) 106099.
[30] Yitao Shen. IOP Conference Series: Earth and Environmental Science, Numerical Study On the Influence of Foamed Copper On Flow Boiling Characteristics, 714, IOP Publishing, 2021 022066.
[31] X. Py, R. Olives, S. Mauran, Paraffin/porous-graphite-matrix composite as a high and constant power thermal storage material, Int. J. Heat Mass Transf. 44 (2001) 2727–2737.
[32] H. Xu, L. Gong, S. Huang, M. Xu, Flow and heat transfer characteristics of nanofluid flowing through metal foams, Int. J. Heat Mass Transf. 83 (2015) 399–407.
[33] C.Y. Wang, C. Beckermann, A two-phase mixture model of liquid-gas flow and heat transfer in capillary porous media-I. Formulation, Int. J. Heat Mass Transf. 36 (1993) 2747–2758.
[34] D.A. Nield, A. Bejan, Convection in Porous Media, Springer International Publishing, 2017. Fourth ed.
[35] W.H. Lee, A Pressure Iteration Scheme For Two-Phase Flow Modeling, in: T. N. Veziroglu (Ed.), Multiphase Transport Fundamentals, Reactor Safety, Applications, (1980) 407–432.
[36] H.I. Mohammed, D. Giddings, G.S. Walker, CFD simulation of a concentrated salt nanofluid flow boiling in a rectangular tube, Int. J. Heat Mass Transf. 125 (2018) 218–228.
[37] LiLi Gao, Lin Zhang, ZhiLei Ma, Chen Xu, ZhangPing Xiao, MingZhao Du, The Numerical Simulation of Flow and Boiling Heat Transfer of Two Phases in Horizontal Tube, in: 2012 Asia-Pacific Power and Energy Engineering Conference, IEEE, 2012, pp. 1–4.
[38] S.C. De Schepper, G.J. Heynderickx, G.B. Marin, Modeling the evaporation of a hydrocarbon feedstock in the convection section of a steam cracker, Comput. Chem. Eng. 33 (2009) 122–132.
[39] X. Li, K. Li, J. Tu, J. Buongiorno, on two-fluid modeling of nucleate boiling of dilute nanofluids, Int. J. Heat Mass Transf. 69 (2014) 443–450.
[40] B. Zheng, Y. Liu, L. Zou, R. Li, Heat transfer characteristics of calcined petroleum coke in waste heat recovery process, Mathem. Prob. Eng. (2016).
[41] Z.G.H.J. Xu, T.S. Wang, W.Q. Tao, T.J. Lu, Thermal Transport in Metallic Porous Media. Heat Transfer-Engineering Applications, Prof. Vyacheslav Vikhrenko (Ed.), (2011)171–204.
[42] Bernardo Buonomo, Anna Di Pasqua, Piera Ginetti, Oronzio Manca, Pore density effect on a heat exchanger in aluminum foam with flat-tubes, in: AIP Conference Proceedings 2191, AIP Publishing LLC, 2019 020030.
[43] Altay Arbak, Nihad Dukhan, Özer Bağcı, Mustafa Özdemir, Influence of pore density on thermal development in open-cell metal foam, Exp. Therm. Fluid Sci. 86 (2017) 180–188.